5th International Science Congress & Exhibition APMAS2015, Lykia, Oludeniz, April 16–19, 2015

Corrosion and Tribocorrosion Behavior of Cast and Machine Milled Co-Cr Alloys for Biomedical Applications

F. Mindivan[a], M.P. Yildirim[b], F. Bayindir[b] and H. Mindivan[c,d,*]

[a]Bilecik S.E. University, Technical Programs Department, Bilecik, Turkey

[b]Ataturk University, Prosthodontics Department, Erzurum, Turkey

[c]Bilecik S.E. University, Mechanical and Manufacturing Engineering Department, Bilecik, Turkey

[d]Bilecik S.E. University, Central Research Laboratory, Bilecik, Turkey

In this study, the electrochemical behavior and tribocorrosion performance of cobalt-chromium (Co-Cr) alloys produced by different fabrication methods (casting and CAD/CAM milling technique) have been investigated in the laboratory-simulated artificial saliva. The results have shown that the maximum tribocorrosion resistance was obtained for milled Co-Cr alloy because of higher corrosion resistance and hardness of milled Co-Cr alloy compared too those of cast Co-Cr alloy. Moreover, the lowest friction coefficient was achieved for milled Co-Cr alloy.

DOI: 10.12693/APhysPolA.129.701

PACS/topics: 81.40.Pq, 82.45.Bb, 87.85.jf

1. Introduction

Co-Cr alloys are satisfactorily accepted as dental implants due to their excellent corrosion resistance, biocompatibility, and low cost [1]. However, during their lifetime Co-Cr based biomedical alloys are subjected to different mechanical actions (friction, abrasion, erosion, etc.), thus resulting in a tribocorrosion, which is a degradation phenomenon of material surfaces as a result of simultaneous action of wear and corrosion [2]. The main quality of Co-Cr alloys is their resistance to tribocorrosion, which may be influenced by the heterogeneity of the surface. The heterogeneity of the surface is also strongly influenced by the manufacturing process of the used implant [1]. Co-Cr structures may be obtained through conventional casting or using CAD/CAM milling systems. In this study, the influence of the manufacturing method (casting, and milling) on the corrosion and tribocorrosion performance of Co-Cr alloys has been investigated.

2. Materials and methods

Cast and milled Co-Cr alloys (see Table I for composition details) were used in this study. Cast and milled Co-Cr alloys correspond to Type III and Type IV, respectively. In accordance with the standard metallographic procedure, grinding up to 1200 mesh and polishing with alumina solution were applied to the studied Co-Cr alloys. Microstructural analysis on the alloys was conducted using examination under optical microscope (OM). Porosity in the alloys was measured by the standard metallographic method (grid intercept technique) as well as by a helium-gas-based pycnometer.

TABLE I

Materials and manufacturing methods.

Method	Material	Composition
Cast	Microlit isi; Type III	61.1% Co, 27.8% Cr, 8.5% W, 1.7% Si
Milled	CopraBond K, Type IV	61% Co, 28% Cr, 8.5% W, 1.65% Si

The hardness of the alloys was measured using Schimadzu HMV2 hardness tester with a Vickers pyramid indenter under indentation load of 100 g. The potentiodynamic polarisation measurements were performed utilizing a typical three electrode potentiodynamic polarization test unit in artificial saliva solution at room temperature. Before potentiodynamic polarization measurements, an initial delay of 45 min was employed in order to measure the open circuit potential between working and reference electrodes. Potentiodynamic polarization curves were generated by sweeping the potential from cathodic to anodic direction at a scan rate of 1 $\mathrm{mV\,s^{-1}}$, from -1 V up to $+1$ V. Corrosion potentials (E_{corr}) and corrosion current densities (i_{corr}) were calculated using a Tafel type fit in the software. A reciprocating motion, tribometer attached to a potentiostat/galvanostat was also used as a tribocorrosion apparatus. The tribocorrosion tests were conducted in a simulated artificial saliva solution at room temperature using the same three-electrode set-up that was used in corrosion tests. The wear tests were performed in a reciprocating mode with a 1.7 $\mathrm{cm\,s^{-1}}$ sliding rate under the applied load of 5 N for 45 min. The counter body was an alumina ball with 10 mm diameter. The choice of alumina ball as the counter body was made because of its high hardness, high wear resistance, chemical inertness and electrical insulating properties. The ball holder was made of a polymeric material to prevent the corrosion effects.

*corresponding author; e-mail: hmindivan@hotmail.com

During the test, alloy with an area of 2 cm^2 was exposed to the corrosive electrolyte. The corrosion and tribocorrosion experiments have been repeated three times for each specimen. The wear tracks were also evaluated by scanning electron microscopy (SEM) coupled with energy dispersive spectroscopy (EDS) and two-dimensional contact profilometer (Surftest SJ 400).

3. Results and discussion

Figure 1 shows OM images of cast and milled Co-Cr alloys for comparison. When compared with the milled Co-Cr alloy (Fig. 1b), relatively coarse micropores are observed in the cast Co-Cr alloy (Fig. 1a). Namely, the porosity of cast and milled Co-Cr alloys was determined as 3% and 0%, respectively. As shown in Fig. 2, the maximum hardness was achieved for milled Co-Cr alloy. It is believed that the presence of intrinsic casting defects such as micropores in cast Co-Cr alloy is the main reason for the decrease of the hardness. The non-uniformity of the structure of the cast Co-Cr alloy was confirmed by the standard deviation of the Vickers microhardness value. Similar to the present result, a few studies reported that casting technique can lead to poor mechanical properties compared to other manufacturing processes such as powder metallurgy and forging [3, 4].

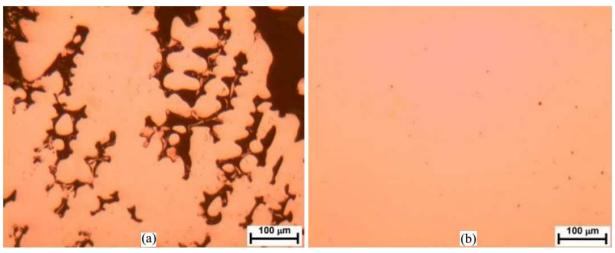

Fig. 1. OM images of the unetched (a) cast and (b) milled Co-Cr alloys.

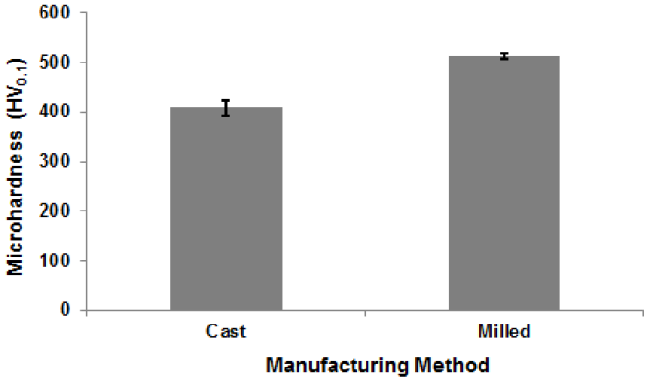

Fig. 2. Microhardness values of Co-Cr alloys according to manufacturing method.

The corrosion resistance of cast and milled Co-Cr alloys was determined in artificial saliva solution using potentiodynamic polarization tests as shown in Fig. 3. It was found that the Tafel curve for milled Co-Cr alloy exhibits a corrosion potential at −394 mV (SCE), which is positively shifted by about 26 mV SCE relative to cast Co-Cr alloy with corrosion potential at −420 mV (SCE). Meanwhile, the corrosion current density of milled Co-Cr alloy was 2.53 $\mu A\,cm^{-2}$, approximately 2.5 times lower than that of cast Co-Cr Alloy (6.31 $\mu A\,cm^{-2}$). The polarisation test results lead directly to the conclusion that the corrosion resistance of milled Co-Cr alloy in artificial saliva corrosive medium was better than that of cast Co-Cr alloy.

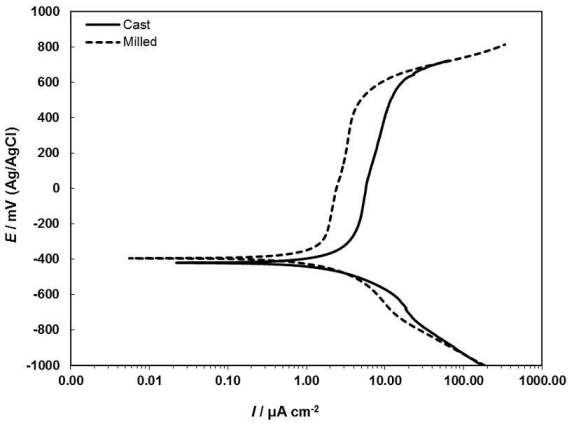

Fig. 3. Potentiodynamic polarisation curves for Co-Cr alloys in a simulated artificial saliva solution.

The surfaces of the Co-Cr alloys after the potentiodynamic polarization experiment were examined using SEM to identify the sites of corrosion attack (Fig. 4). The SEM images show that the corrosion attack in the cast Co-Cr alloy take place predominantly by pitting corrosion (Fig. 4a). EDS analysis of the corroded areas indicates severe depletion of cobalt from the matrix. Similar to the present result, a few studies reported that corrosion of Co-Cr alloys occurred through selective dissolution of Co-rich regions [5, 6]. In the case of the milled Co-Cr alloy, the surface remains the same without any visible change (Fig. 4b). Lower corrosion resistance and higher metal release for the cast Co-Cr alloy compared with the milled Co-Cr alloy can be attributed to local variations in composition and the heterogeneous microstructure.

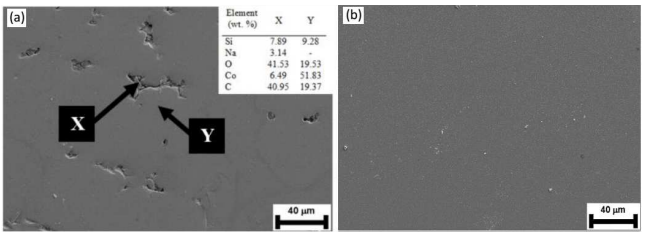

Fig. 4. SEM images and EDS analysis of (a) cast and (b) milled Co-Cr alloys after polarization test.

The evolution of the open circuit potential (OCP) with time before, during, and after the sliding are given in Fig. 5 for cast and milled Co-Cr alloys, together with the friction coefficient values obtained during the sliding. When rubbing is started, the OCP shifts towards the cathodic values (−450 mV vs SCE in cast Co-Cr alloy, −440 mV vs SCE in milled Co-Cr alloy) when compared to the initial potential (−290 mV vs SCE in cast Co-Cr alloy, −350 mV vs SCE in milled Co-Cr alloy). When the evolution of OCP is considered (Fig. 5a), it can be seen that the milled Co-Cr alloy presented a smaller drop of the potential on the onset of the sliding, as compared to the cast Co-Cr alloy. Thus, the OCP drop reflects the extent of depassivation caused by the counter body [7]. Once rubbing stops, depassivation ceases and the OCP recovers the initial value established before rubbing. Similar behavior has also been reported in the literature [8]. On the other hand, Fig. 5b shows the evolution of the friction coefficient with number of cycles for the cast and milled Co-Cr alloys under the lubrication with saliva solution. As can be seen, the friction coefficient of cast Co-Cr alloy starts high and then decreases to the steady values after about 30 running cycles, however the milled Co-Cr alloy presented relatively stable average friction coefficient values during the sliding and possesses lower friction coefficient than the cast Co-Cr alloy.

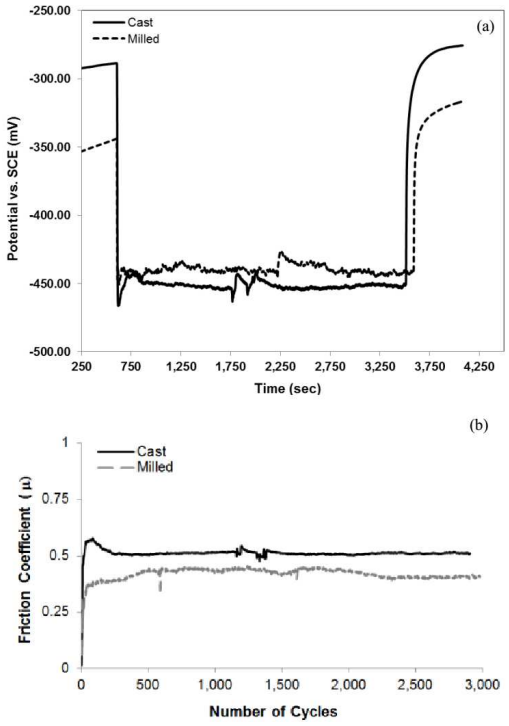

Fig. 5. The evolution of the (a) OCP and (b) friction coefficient values obtained during sliding.

Figure 6 shows representative SEM images of the worn surfaces of cast and milled Co-Cr alloys at the end of the tribocorrosion test. Sliding grooves were observed on the cast Co-Cr alloy, indicating abrasive wear that can be occurring due to the penetration of the asperities on the counter material (Fig. 6a). Similar wear mechanism was reported by Ribeiro et al. in [9], where the synergistic effect of corrosion and wear for CoCrMo-Al_2O_3 composites was investigated. In comparison, the worn surface topography of the milled Co-Cr alloy was very smooth (Fig. 6b).

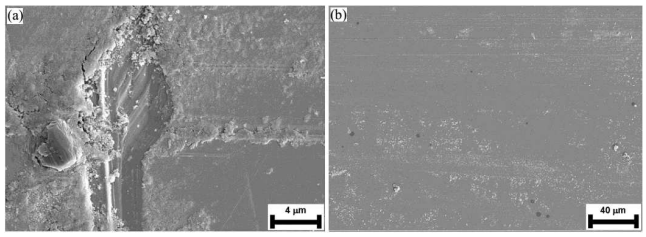

Fig. 6. SEM pictures of the wear tracks after the tribocorrosion test of (a) cast and (b) milled Co-Cr alloys.

The alumina balls were investigated using OM to identify possible damage. No alumina wear could be observed, but some wear debris was observed on the surface of the alumina ball rubbing against cast Co-Cr, as shown in Fig. 7a. No material transfer from the milled Co-Cr alloy was observed on the alumina ball (Fig. 7b).

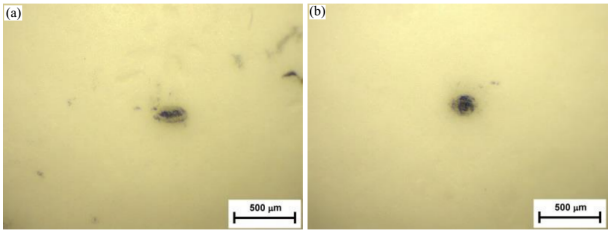

Fig. 7. OM images of the alumina balls rubbing against (a) cast and (b) milled Co-Cr alloys.

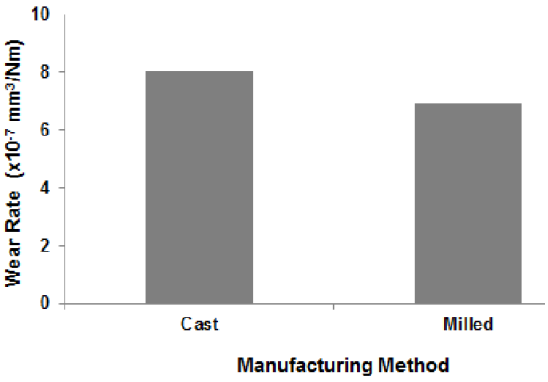

Fig. 8. Wear rate values after tribocorrosion tests.

The wear rate values after tribocorrosion tests are presented in Fig. 8. As shown in Fig. 8, the wear rate of the cast Co-Cr alloy was bigger than that of the milled Co-Cr alloy. It seems that the higher corrosion resistance and hardness of milled Co-Cr alloy compared to those of cast Co-Cr alloy are the main reasons for the higher tribocorrosion resistance.

4. Conclusions

The conclusions of this study conducted on the cast and milled Co-Cr alloys are as follows:

1. Potentiodynamic polarisation curves for Co-Cr alloys in artificial saliva solution have shown that cast Co-Cr alloy was more susceptible to localised corrosion.

2. The hardness, corrosion resistance values and tribocorrosion performance of milled Co-Cr alloy are satisfactory and this material seems to be suitable for application.

Acknowledgments

The financial support of the research foundation of Bilecik S.E. University is gratefully acknowledged. The authors would also like to thank S. Temel and O. Gokmen from the Central Research Laboratory of Bilecik S.E. University for their technical support.

References

[1] V.S. Saji, H.C. Choe, *Trans. Nonferrous Met. Soc. China* **19**, 785 (2009).

[2] M.A. Arenas, A. Conde, J.J. DE Damborenea, *Metall. Mater. Trans. A* **44**, 4382 (2013).

[3] J.V. Giacchi, C.N. Morando, O. Fornaro, H.A. Palacio, *Mater. Charact.* **62**, 53 (2011).

[4] Z. Doni, A.C. Alves, F. Toptan, J.R. Gomes, A. Ramalho, M. Buciumeanu, L. Palaghian, F.S. Silva, *Mater. Design* **52**, 47 (2013).

[5] X. Zhang, Y. Li, N. Tang, E. Onodera, A. Chiba, *Electrochim. Acta* **125**, 543 (2014).

[6] Y.S. Hedberg, B. Qian, Z. Shen, S. Virtanen, I.O. Wallinder, *Dent. Mater.* **30**, 525 (2014).

[7] M.P. Licausi, A.I. Munoz, V.A. Borras, *J. Mech. Behav. Biomed.* **20**, 137 (2013).

[8] T. Kosec, P. Mocnik, A. Legat, *Appl. Surf. Sci.* **288**, 727 (2014).

[9] A.M. Ribeiro, A.C. Alves, L.A. Rocha, F.S. Silva, F. Toptan, *Tribol. Int.* **91**, 198 (2015).